

Performance Verification of the Ground-Based Mid-Infrared Camera MAX38 on the MiniTAO Telescope

Kentaro Asano^{*a}, Takashi Miyata^a, Shigeyuki Sako^a, Takafumi Kamizuka^a, Tomohiko Nakamura^{ab}, Mizuho Uchiyama^a, Mizuki Yoneda^c, Hirokazu Kataza^d, Yuzuru Yoshii^a, Mamoru Doi^a, Koutaro Kohno^a, Kimiaki Kawara^a, Masuo Tanaka^a, Kentaro Motohara^a, Toshihiko Tanabe^a, Takeo Minezaki^a, Tomoki Morokuma^a, Yoichi Tamura^a, Tsutomu Aoki^e, Takao Soyano^e, Kenichi Tarusawa^e, Natsuko Kato^a, Masahiro Konishi^a, Shintaro Koshida^a, Hidenori Takahashi^a, Toshihiro Handa^f, Ken Tateuchi^a

^aInstitute of Astronomy, The University of Tokyo, Osawa 2-21-1, Mitaka, Tokyo 181-0015, Japan;

^bDepartment of Astronomy, The University of Tokyo, Hongo 7-3-1, Bunkyo, Tokyo 113-0033, Japan;

^cAstronomical Institute, Tohoku University, Aramaki 6-3, Aoba-ku, Sendai, Miyagi 980-8578, Japan;

^dInstitute of Space and Astronautical Science, Yoshinodai 3-1-1, Chuo-ku, Sagamihara, Kanagawa 252-5210 Japan;

^eKiso Observatory, University of Tokyo, Mitake 10762-30, Kiso, Nagano 397-0101, Japan;

^fFaculty of Science, Kagoshima University, Korimoto 1-21-24, Kagoshima Japan

ABSTRACT

We have evaluated on-sky performances of a mid-infrared camera MAX38 (Mid-infrared Astronomical eXplorer) on the miniTAO 1-meter telescope. A strehl ratio at the N-band is estimated to be 0.7-0.8, and it reaches to 0.9 at the 37.7 micron, indicating that diffraction limited angular resolution is almost achieved at the wavelength range from 8 to 38 micron. System efficiencies at the N and the Q-band are estimated with photometry of standard stars. The sensitivity at the 30 micron cannot be exactly estimated because there are no standard stars bright enough. We use the sky brightness instead. The estimated efficiencies at the 8.9, 18.7, and 31.7 micron are 4%, 3%, 15% , respectively. One-sigma sensitivity in 1 sec integration of each filter is also evaluated. These give good agreements with the designed values. Preliminary scientific results are briefly reported.

Keywords: mid-infrared, ground-based instrument, camera, TAO

1. INTRODUCTION

Mid-infrared wavelengths of 25–40 micron are one of the most important wavelengths to observe dusty astronomical objects such as star forming regions, mass losing stars, and planetary/debris disks. This wavelength includes a wide variety of dust feature in addition to the peak of the blackbody radiation of $\sim 100\text{K}$, which is comparable to temperature of circumstellar dust shells/disks and dusty galaxies.

Many of space telescopes including IRAS, ISO, Spitzer, and Akari have been used for the mid-infrared observations. Although these achieve excellent sensitivity, spatial resolution is unsatisfied because of their limited size of primary mirrors. Short lifetime and highly competitive observing time is another problem of the space telescopes especially for carrying out monitoring observations.

Ground-based telescopes, on the other hand, can achieve higher spatial resolution. Some instruments working at the N-band (at 10 micron) and the Q-band (at 20 micron) have produced a lot of remarkable results so far.

Further author information: (Send correspondence to K.Asano)

K.Asano: E-mail: kenasano@ioa.s.u-tokyo.ac.jp, Telephone: +81 422 34 5163

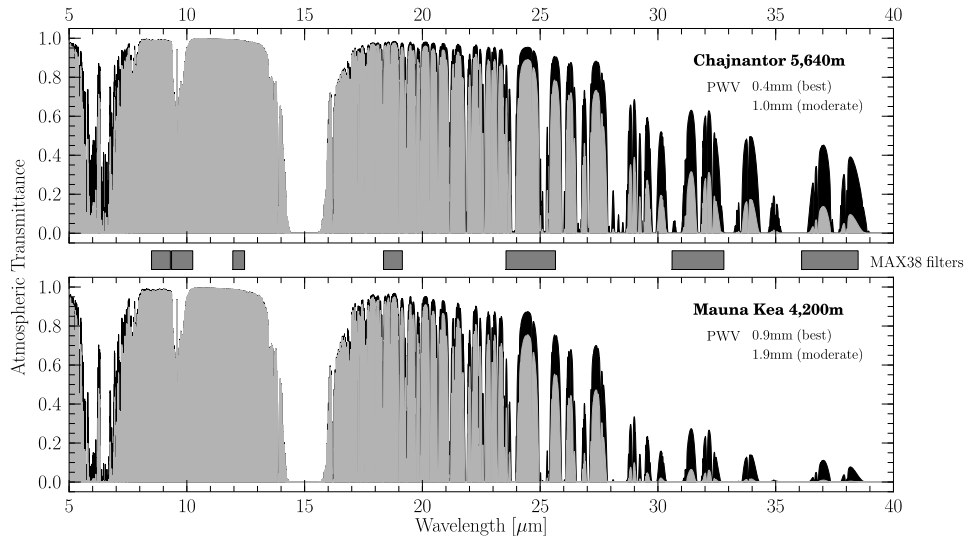


Figure 1. Atmospheric transmittances in the mid-infrared wavelength at the Chajnantor TAO site and Mauna-Kea site simulated using ATRAN atmospheric model (Lord 1992^[4]). Black solid lines represent atmospheric transmittance curves at the best PWV (0.4 and 0.9 mm respectively) of each site, while gray lines represent ones at a moderate PWV (1.0 and 1.9 mm respectively) of each site. The boxes between upper and lower panel represent wavelength regions which MAX38 filters cover.

However instruments which cover the wavelength range of 25–40 micron have not existed because stellar emissions in these wavelengths are heavily absorbed by the atmosphere.

We have developed a mid-infrared camera MAX38 (Mid-infrared Astronomical eXplorer; Miyata et al. 2008^[1]) for observations at 8–38 micron. It is mounted on the University of Tokyo Atacama 1.0-m(miniTAO) telescope (Sako et al. 2008^[2]) at the summit of Co.Chajnantor in Northern Chile. This is a pathfinding telescope of the Tokyo Atacama Observatory (TAO; Yoshii et al. 2010^[3]), which is project to build a 6.5m- infrared-optimized telescope. An extremely high altitude of 5,640m and dry weather conditions enable us to access the 30 micron wavelength region.

MAX38 achieved the first light observations in October 2009 (Nakamura et al. 2010^[5]) and had four observing runs. In this paper we report on-sky performances of MAX38. The evaluated performance such as point spread functions and system efficiency, and sensitivity are described in section 2. First science results of MAX38 are described in section 3. Finally, we summarize of this work in Section 4.

2. PERFORMANCE VERIFICATION

2.1 Point Spread Function

Spatial resolution is a key parameter for the ground-based observation at the mid-infrared. We evaluate it as a point spread function (PSF) based on images of stars for each filter listed in Table 1.

2.1.1 N / Q band

For the evaluations of the PSFs in the N and the Q-bands, a bright post-supergiant IRC+10420 was observed in 8th November 2011. Since it is surrounded by a dust shell it is not exactly a point source in the mid-infrared. The radius of the shell was estimated to be less than 300 mas (Blöker et al 1999^[6]) which is much smaller than the spatial resolution of MAX38. Thus we regard it as a point source. The sky condition at the observations was clear and stable. We carried out observations with the integration time of 2.6 sec for each filter. Data was analyzed with standard tasks of IRAF software.

The measured PSFs are displayed in Figure 3. They have nearly round-shapes with diffraction rings. The full width of half maximum of the PSFs at 8.9, 9.8, 11.2, and 18.7 micron filters are 2.4, 2.7, 3.2 and 4.9 arcsec, respectively. They almost comparable to the diffraction limited values. (see Table 1).

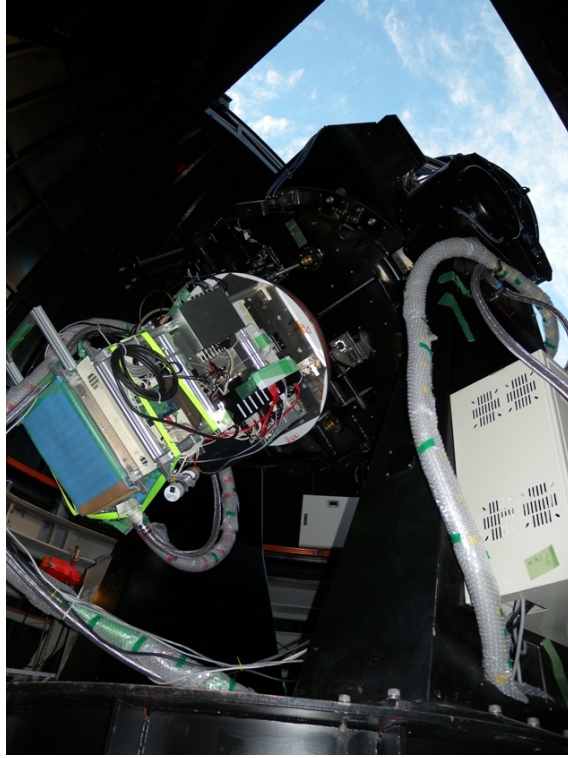


Figure 2. MAX38 on the miniTAO telescope. MAX38 is mounted on the Cassegrain focus of the telescope.

2.1.2 30 micron bands

For the evaluation in the 30 micron wavelength range, a red supergiant VY CMa was observed. It is one of the brightest sources at the mid-infrared. This is also known as an extended object. Wittkowski et al (1998)^[7] suggests that VY CMa has a non-spherical shape in the K-band. Its size of 200 mas is negligible for the present evaluations because the diffraction limited spatial resolution of MAX38 in the 30 micron is expected to be approximately 8 arcsec. The observation was carried out under excellent condition with the perceptible water vapor (PWV) of 0.4 mm in 6th Nov 2011. Integration time was 25 sec for each filter.

The observed PSFs are shown in Figure 3. They show clear diffraction rings. The strehl ratio is estimated to be 0.8 and 0.9 at the 31.7 and 37.7 micron, respectively. These demonstrate that they almost perfectly achieved the diffraction limited spatial resolution.

Name	Central wavelength [μm]	Bandwidth [μm]	Measured FWHM [arcsec]	diffraction limit [μm]	strehl ratio
J089W08	8.9	0.8	2.39	2.19	0.74
J098W09	9.8	0.9	2.65	2.41	0.71
J122W05	12.2	0.5	3.15	3.00	0.78
R187W09	18.7	0.9	4.91	4.60	0.80
MMF31	31.7	2.2	7.56	7.79	0.84
MMF37	37.3	2.4	8.51	9.17	0.93

Table 1. comparison of MAX38 measured PSF and diffraction limit , and strehl ratio.

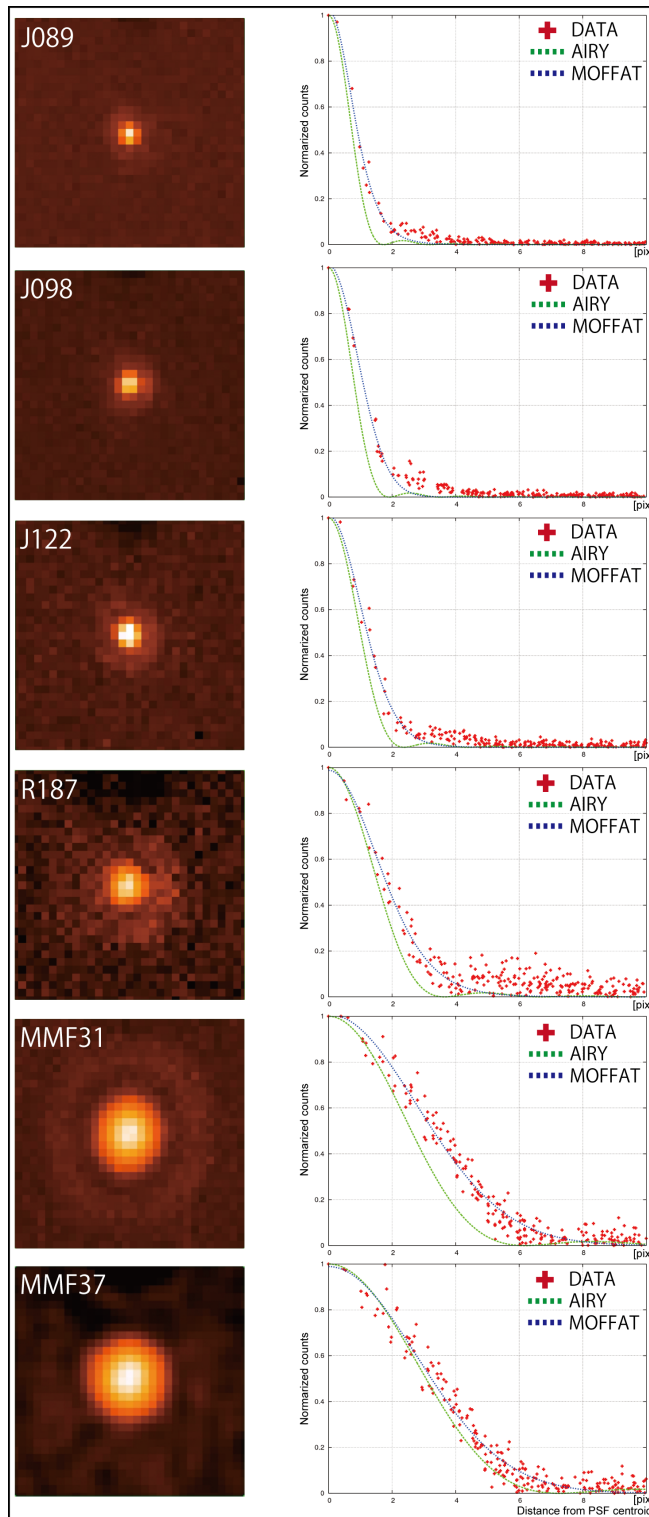


Figure 3. An image of a star (left panels) and its radial profile (right panels) of each MAX38 filter. Size of the images are 30×30 pixels, and pixel scale of MAX38 is 1.26 arcsec/pix. In right panels, observed radial profiles are shown by cross, while Moffat functions fitted to data is shown by blue dotted lines. Airy functions calculated from optical design with green dotted line.

2.2 System efficiency of MAX38

The system efficiency of MAX38, τ_{cam} , is defined as

$$\tau_{\text{cam}} = \tau_{\text{opt}} \cdot \tau_{\text{fil}}(\lambda) \cdot \eta G(\lambda) d\lambda \quad (1)$$

where τ_{opt} is the throughput of the optics including inner mirrors and an entrance window, τ_{fil} is the filter transmittance, and $\eta G(\lambda)$ is the quantum efficiency of the detector. We note that τ_{cam} does not include the atmospheric transmittance τ_{atm} and the telescope reflectance τ_{tel} .

2.2.1 N-band / Qband

The system efficiency is estimated from photometric measurements of standard stars by the following equation:

$$P_{*\text{exp}} = \int F_*(\lambda) \cdot \tau_{\text{atm}} \cdot \tau_{\text{tel}} \cdot \tau_{\text{cam}} d\lambda \quad (2)$$

where $P_{*\text{exp}}$ is a detected photocurrent from a star, and $F_*(\lambda)$ is an intrinsic flux of the star.

Standard stars 24 Cap, α Tuc, and Pi2 Aqr are used for the estimation of the system efficiency in the N and the Q bands. Observations were carried out in 7th Nov 2011. Integral time is typically 50 sec and 1,000 sec in the N and the Q-bands, respectively, to achieve sufficient signal-to-noise ratios. The sky condition was good enough for the photometry. The PWV was approximately 0.5 mm during the observations.

We assume that the throughput of the telescope τ_{tel} as 0.7 based on measurement of the reflectivity of the primary mirror in the optical wavelength. The atmospheric transmittance τ_{atm} is calculated from ATRAN model (LORD et al. 1992) with an altitude of 5,640m and the PWV of 0.5 mm. The intrinsic fluxes of the stars are provided by Cohen et al. (1999)^[8].

The evaluated system efficiencies are tabulated together with the assumptions in Table 2. These fall within the range of 3-5%. Reliability of the results is discussed in section 2.2.3.

2.2.2 Thirty micron windows

Since the sky is incredibly unstable in the 30 micron wavelength region, it is quite difficult to estimate the system efficiency based on the photometry of stars. Figure 4 shows a sample of apparent brightness of a star eta Car measured at the 31.7 micron. Its brightness varies more than 10% in a few minutes and more than 700% in a few hours. This could be an extreme one but the variation with a factor of two is usually observed (see also Miyata et al. 2012a^[9]).

The apparent brightness of the star is found to be clearly correlated with brightness of the sky background (Figure 5). This is naturally explained by time variation of the atmospheric transmittance: the brightness of the star increases and the brightness of the sky decreases when the sky gets more transparent, and vice versa. The data are fit with a linear function. The x-interception of the fitted line corresponds to the brightness of the sky when the sky is completely opaque. In this case the photocurrent P_{atm} is calculated by the following equation.

$$P_{\text{atm}} = \int B_{\text{sky}}(T_{\text{atm}}, \lambda) \cdot \epsilon_{\text{atm}} \cdot \tau_{\text{tel}} \cdot \tau_{\text{opt}} \cdot \tau_{\text{fil}}(\lambda) \cdot \eta G(\lambda) d\lambda \quad (3)$$

Here B_{sky} is a blackbody radiation of the sky. It is to be noted that the value of the x-interception (9.98×10^8 e⁻/s) includes the thermal emission from the telescope and the entrance window of MAX38. These are estimated as grey body radiations with some assumptions tabulated in Table 2. The system efficiencies evaluated with the equation 3 are shown in Table 3.

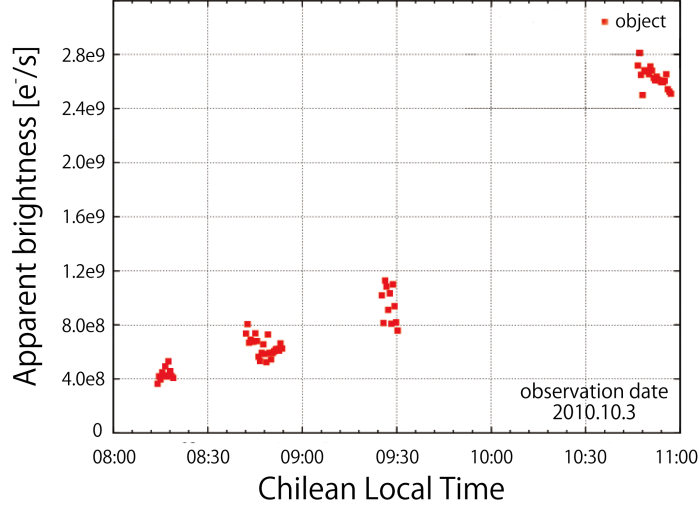


Figure 4. A sample of a strong sky variation. A horizontal and a vertical axes shows an observation time in Chilean local time and an apparent brightness of a star η Car at 31 micron. The apparent brightness varied 700% in a few hours.

2.2.3 Wavelength dependence of the system efficiency

The estimated system efficiency at the 31.7 micron is about 3-5 times higher than the efficiencies at the N-band. It is reasonably explained by wavelength dependence of the quantum efficiency. In the equation (1) the throughput of the optics is calculated as the multiplication of reflectance of the mirrors (0.98 for each mirror) and the throughput of the window (0.7). The filter transmittances were measured ahead in a laboratory. Therefore we can estimate the quantum efficiency of the detector from the system efficiency.

The results are listed in column 5 of Table 3. The quantum efficiency is 5-10 % at the N-band and it increases with the wavelength. It shows a peak of 64% around the 30 micron and rapidly decreases between 30 and 38 micron. This wavelength dependence is consistent with the results of laboratory measurements provided by the DRS.

Parameter	Value
Sky temperature (estimated)	260K
Sky emissivity	100%
Telescope emissivity (estimated)	30 %
Telescope temperature	260 K
Window transmission	70%
Window emissivity	2%
Window temperature (estimated)	260 K
Primary mirror diameter	1.024 m
pixel size	75 μ m
pixel scale	1.26 arcsec/pix
conversion factor	200 e ⁻ /ADU

Table 2. Typical parameters used for the point source sensitivity model.

2.3 Sensitivity of MAX38

2.3.1 N-band / Qband

The sensitivity of N-band (8.9, 9.8, 12.2 micron) and Q-band (18.7 micron) are estimated from photometric measurements of stars, for example 24 CAP. Details of the observations and the stars were described in section

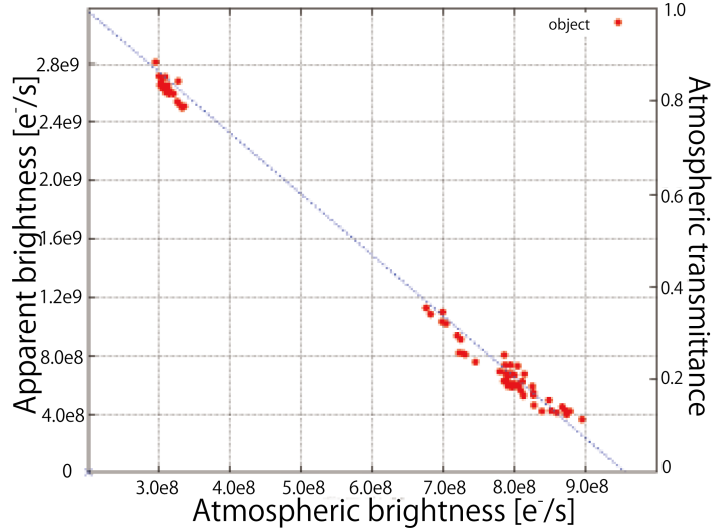


Figure 5. A relation between the atmospheric brightness and the apparent brightness of a star at 31.7 micron. Filled circles represents the observed data and a dotted line represents a fitted line derived from least square method. A clear correlation between apparent brightness and atmospheric brightness is displayed.

2.2. Aperture photometry with a circular aperture is applied. The aperture radii at 8.9, 9.8, 12.2, and 18.7 micron are set to be 2.5, 3, 3, 4 arcsec, respectively. Errors of the photometry are calculated as standard deviations of the background counts around the stars. The estimated 1-sigma sensitivities in 1 second are listed in Table 3. These are almost comparable with the expected sensitivities in Miyata et al 2008^[1].

2.3.2 30 micron bands

The sensitivity of 30 micron bands are estimated from photometric measurements of α Ori. There are not standard star at 30 micron. α Ori is a one of the most famous variable stars. It is an irregular pulsating variable that exhibit changes in magnitude from 0.2 to 1.2 in visible.

Monnier et al. (1998)^[10] pointed out that its brightness in the mid-infrared wavelengths is expected to be almost stable. He obtained N-band spectra of α Ori 7 times from 1994 to 1997, and suggested that the brightness at the N-band changed less than 10%. We use the data of the intrinsic flux at 30 micron band with ISO spectrum. Its flux is about 900 Jy at 31.7 micron, about 630 Jy at 37.7 micron.

The observations at the 31.7 micron and the 37.7 micron were carried out in 8th and 9th Nov. 2011. These were clear nights with the PWV of ~ 0.4 mm. Integration time for each filters are 100 seconds (31.7micron) and 600 seconds (37.7 micron). The airmass at the observations was 1.27.

Aperture photometries with an aperture radius of 5 arcsec are applied, and errors are estimated from the sky counts around the star. The 1-sigma sensitivity in 1 sec at the 31.7 and 37.7 micron are estimated to be 28 and 70 Jy, respectively.

These are approximate three or four times larger than the expected sensitivities. This may be caused by the difference of the atmospheric transmittance. Miyata et al. (2008) estimated the sensitivities under the assumption of the PWV ~ 0.19 mm, while the observations were carried out under the condition of the PWV ~ 0.4 mm. The transmittance of the thirty micron windows is expected to dramatically improve in these PWV range.

3. FIRST SCIENCE RESULTS

3.1 31 micron observation : New Detection of Cold Dust Component in PN, Mz3

Mz3 is one of the famous bipolar planetary nebulae surrounded a massive dust shell. So far a lot of studies have been performed to reveal spatial distributions of the dust in the nebula. Smith et al. (2005) carried out

Name	Central wavelength [μm]	Atmosphere transmittance	Filter transmittance	Detector sensitivity [%]	System efficiency [%]	Sensitivity [$\text{Jy}/1\sigma 1\text{sec}$]
J089W08	8.9	0.9	0.85	6.9	3.37	1.7
J098W09	9.8	0.60	0.90	5.4	2.76	2.8
J122W05	12.2	0.75	0.85	12	5.27	3.1
R187W09	18.7	0.82	0.50	14	3.33	2.2
MMF31	31.7	0.33	0.40	64	14.7	28
MMF37	37.3	0.23	0.40	32	5.45	70

Table 3. System Efficiency of MAX38, not including the atmosphere and the telescope.

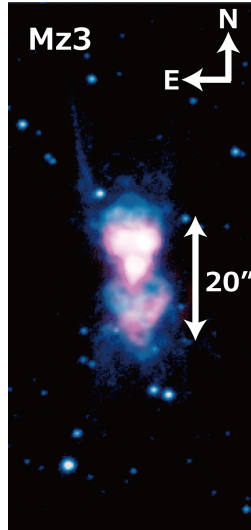


Figure 6. Bipolar planetary nebula Mz3 observed by miniTAO (red, 31micron MAX38; blue, Pa α a near infrared camera on miniTAO telescope(ANIR)). A color version of this figure is available in the electronic edition.

imaging observations with a high spatial resolution at the N and the Q-band, and found that warm ($T\sim 300\text{K}$) dust components in Mz3 concentrate to a central region of the nebula. However the distribution of relatively cold component, which corresponds to most of the dust mass, has remained unclear yet. We have obtained an image of Mz3 at the 31.7 micron with a spatial resolution of 8 arcsec (Figure 6), which is the highest resolution ever achieved (Asano et al. 2012b). A sufficient amount of the cold dust is surprisingly distributed near the central star. This demonstrates that the observation at the 30 micron is a powerful tool for exploring the cold regions in the Universe. Details of the results are shown in Asano et al. (2012b).

3.2 Monitoring observation : Asteroid 2005YU Closest Approach

Asteroid 2005YU55 is one of near-earth asteroids which are potentially hazardous to human beings. It made an exceptionally close approach to the Earth, passing within 0.0217 AU (325,000km) on 2011-Nov-08 23:24. Such a closest approach was incredibly rare event and a valuable opportunity to study the near earth asteroids in detail. We carried out monitoring observations of the asteroid during the closest approach, and obtained a light curve at the 18.7 micron (Figure 7). This result is very useful for studying the physical parameters of the asteroid. Details have been reported in Miyata et al. 2012b^[12].

4. SUMMARY

We evaluated on-sky performance verification of miniTAO/MAX38 with an altitude of 5,640m, such as PSF, system efficiency, and sensitivity. PSF of each MAX38 filters almost perfectly achieved the diffraction limited spatial resolution. We confirmed the consistency between the system efficiency of measured values and design

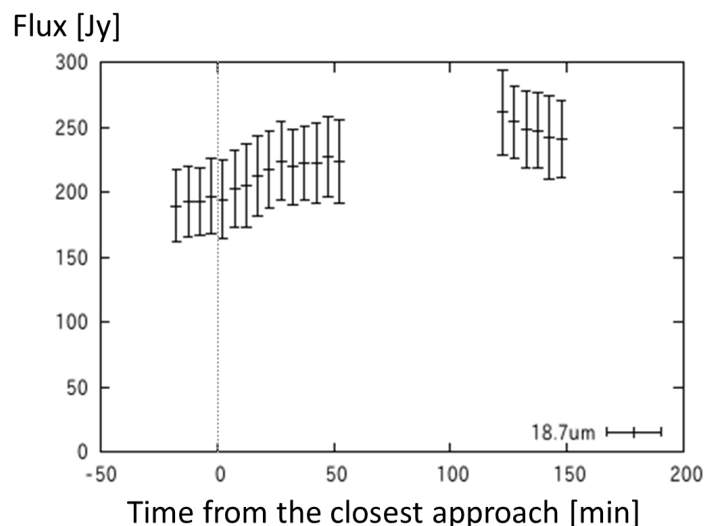


Figure 7. Time variation of a near earth asteroid 2005YU55 observed at 18.7 micron during the closest approach in 8th Nov. 2011.

values. The on-sky measured values of sensitivity at N/Q band is good, while 30 micron are worse than expected values, this is because its values strongly depend on sky conditions.

We show the 30 micron observations a powerful tool for exploring the cold regions in the Universe.

Acknowledgments

This research was supported by MEXT/JPS Grant-in-Aid for Scientific Researches (A) No.22253002 (P.I. Yoshii Y.), and Grant-in-Aid for Young Scientist (A) No. 21684006 (P.I. Miyata, T.) and in part, by a grant from the Hayakawa Satio Fund awarded by the Astronomical Society of Japan. The mini-TAO telescope operates in the Parque Astronomico Atacama in northern Chile under the auspices of Programa de Astronomia, a program of the Comision Nacional de Investigacion Cientificia y Tecnologica de Chile (CONICYT).

REFERENCES

- [1] Miyata, T., et al., "MAX38: A new mid-infrared camera for ground-based 30 micron observations", Proc. SPIE 7014, 701428 (2008)
- [2] Sako, S., et al., "The University of Tokyo Atacama 1.0-m telescope", Proc. SPIE 7012, 70122T (2008)
- [3] Yoshii, Y., et al., "The University of Tokyo Atacama Observatory 6.5m telescope project", Proc. SPIE 7733, 773308 (2010)
- [4] Load et al, Nasa Technical Memo. 103957 (1992)
- [5] Nakamura, T., et al., "MiniTAO/MAX38 first light: 30-micron band observations from the ground-based telescope", Proc. SPIE 7735, 773561 (2010)
- [6] Blöcker, T., et al, "The rapidly evolving hypergiant IRC +10 420: High-resolution bispectrum speckle-interferometry and dust-shell modelling", Astronomy and Astrophysics, v.348, p.805-814, (1999)
- [7] Wittkowski, M., et al, "Diffraction-limited speckle-masking interferometry of the red supergiant VYCMa*", Astronomy and Astrophysics, v.340, L39-42, (1998)
- [8] Cohen, M., et al., "Spectral Irradiance Calibration in the Infrared. X. A Self-Consistent Radiometric All-Sky Network of Absolutely Calibrated Stellar Spectra", Astronomical Journal, 117, 1864 (1999)
- [9] Miyata, T., et al., "Evaluations of new atmospheric windows at thirty micron wavelengths for astronomy", in this conference (2012)

- [10] Monnier, J. D., et al., "Temporal Variations of Midinfrared Spectra in Late-Type Stars", *Astrophysical Journal* 502, 833 (1998)
- [11] Smith, N., et al., "Bipolar Symbiotic Planetary Nebulae in the Thermal Infrared: M2-9, Mz 3, AND He 2-104", *Astrophysical Journal* 129:969-978 (2005)
- [12] Miyata, T., et al., 2012, "Thermal infrared observations of an asteroid 2005 YU55 during the closest approach", *Asteroid, Comets, Meteors meeting* (2012)